International Journal of Advance Research in Science and Engineering
Vol. No.5, Issue No. 11, November 2016
www.ijarse.com
IJARSE
ISSN (O) 2319 - 8354
ISSN (P) 2319 - 8346

NUMERICAL INVESTIGATIONS ON THE SINGLE POINT INCREMENTAL FORMING OF 60-40 BRASS TO FABRICATE HYPERBOLIC CUPS

[1]T. Manohar Reddy, A. Chennakesava Reddy[2]

[1]PG Student, [2]Professor

Department of Mechanical Engineering, JNT University, Hyderabad-500085, (India)

ABSTRACT

The purpose of the current project work was to determine the formability of brass to fabricate hyperbolic cups using single point incremental forming (SPIF) process. The finite element analysis has been carried out to model the single point incremental forming process using ABAQUS software code. The process parameters of SPIF were sheet thickness, step depth, tool radius and coefficient of friction. The process parameters have been optimized using Taguchi techniques. The major process parameters influencing the SPIF of hyperbola cups were step size, tool radius and coefficient of friction.

***Keywords:** Brass, Hyperbolic Cup, Single Point Incremental Forming, Finite Element Analysis, Step Depth, Tool Radius, Sheet Thickness, Coefficient of Friction.*

I. INTRODUCTION

In the deep drawing process, a punch pushes a sheet metal blank into a die cavity, resulting in a contoured part. A part is said to be deep drawn if the depth of the part is at more than half of its diameter. The greater the die cavity depth, the more blank material has to be pulled down into the die cavity and the greater the risk of wrinkling in the walls and flange of the part [1]. In a series of research on deep drawing process to fabricate variety of cup shapes, rich investigation have been carried out to improve the superplastic properties of materials such as AA1050 alloy [2], AA2219 alloy [3], AA3003 alloy [4], Ti-Al-4V alloy [5], EDD steel [6], gas cylinder steel [7]. In SPIF process (figure 1), the sheet material is clamped along its edges and a hemispherical headed tool is moved along a predefined geometrical path so that it deforms the sheet locally along the path. The important process parameters, which influence the SPIF process capability, are tool diameter, step depth, feed rate, rotational speed of the spindle, sheet thickness, lubrication and tool path [8-13]. The present work was to study the formability of hyperbolic cups of 60-40 brass using SPIF. For this purpose, the design of experiments was executed as per Taguchi technique. The process parameters of SPIF were sheet thickness, step depth, tool radius and coefficient of friction. The formability was evaluated using finite element method.

International Journal of Advance Research in Science and Engineering
Vol. No.5, Issue No. 11, November 2016
www.ijarse.com
IJARSE
ISSN (O) 2319 - 8354
ISSN (P) 2319 - 8346

II. MATERIAL AND METHODS

In the present work, ABAQUS (6.14) software code was used for the numerical simulation of SPIF process to fabricate hyperbolic cups. The material was brass. The SPIF process parameters were chosen at three levels as summarized in table 1. The orthogonal array (OA), L9 was preferred to carry out experimental and finite element analysis (FEA) as given in table 2.

Table 1: Process parameters and levels

Factor	Symbol	Level–1	Level–2	Level–3
Sheet thickness, mm	A	0.8	1.0	1.2
Step depth, mm	B	0.50	0.75	1.00
Tool radius, mm	C	4.0	5.0	6.0
Coefficient of friction	D	0.125	0.15	0.175

The sheet and tool geometry were modeled as deformable and analytical rigid bodies, respectively, using ABAQUS. They were assembled as frictional contact bodies. The sheet material was meshed with S4R shell elements. The fixed boundary conditions were given to all four edges of the sheet. The boundary conditions for tool were x, y, z linear movements and rotation about the axis of tool. True stress-true strain experimental data were loaded in the tabular form as material properties. The tool path geometry was generated using CAM software [14] was imported to the ABAQUS as shown in figure 1. The elastic-plastic deformation analysis was carried out for the equivalent stress, strain and strain rates and thickness variation.

Table 2: Orthogonal Array (L9) and control parameters

Treat No. No.	A	B	C	D
1	1	1	1	1
2	1	2	2	2
3	1	3	3	3
4	2	1	2	3
5	2	2	3	1
6	2	3	1	2
7	3	1	3	2
8	3	2	1	3
9	3	3	2	1

International Journal of Advance Research in Science and Engineering
Vol. No.5, Issue No. 11, November 2016
www.ijarse.com
IJARSE
ISSN (O) 2319 - 8354
ISSN (P) 2319 - 8346

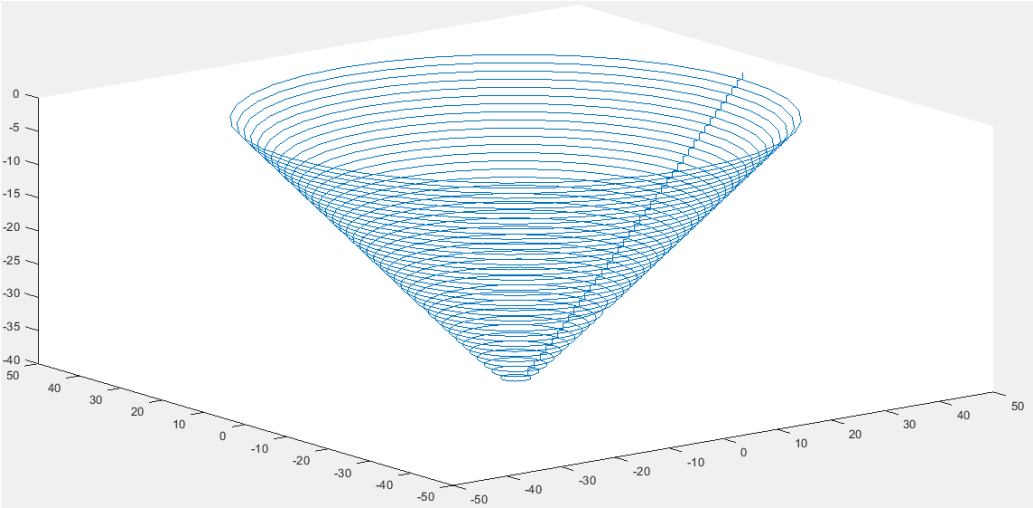

Figure 1: Tool path generation.

III. RESULTS AND DISCUSSION

The influence of process variables on the von Mises stress, strain rate and thickness reduction are discussed. The formability limit diagrams are also constructed.

3.1 Influence of process parameters on effective stress

Table – 3 gives the ANOVA (analysis of variation) summary of von Mises stress data. The percent contribution specifies that sheet thickness, A, contributes 9.39%, step depth, B, accords 30.82%, tool radius, C, presents 42.12% and coefficient of friction, D, attributes 17.67% of total variation on the von Mises stress.

Table 3: ANOVA summary of the effective stress

Source	Sum 1	Sum 2	Sum 3	SS	v	V	P
A	1364.02	1559.61	1363.06	8543.31	2	4271.65	9.39
B	1195.31	1511.83	1579.54	28044.27	2	14022.13	30.82
C	1678.85	1200.77	1407.05	38332.18	2	19166.09	42.12
D	1333.99	1344.55	1608.14	16083.07	2	8041.54	17.67
e				0.00	0		0.00
T	5572.17	5616.76	5957.78	91002.82	8		100.00

IJARSE
ISSN (O) 2319 - 8354
ISSN (P) 2319 - 8346

Note: *SS is the sum of square, v is the degrees of freedom, V is the variance, P is the percentage of contribution and T is the sum squares due to total variation.*

Fig.2a presents the influence of sheet thickness and step depth on von Mises stress induced in brass. The von Mises stress is increased initially with increase of sheet thickness up to 1.00 mm (Fig.2a) and later on, it decreases with sheet thickness from 1.00 mm to 1.2 mm. The von Mises stress increases with increasing of the step size. The effective stress was low for tool radius of 5 mm as shown in Fig.2b. The effective stress is increased with the coefficient of friction as shown in Fig2b.

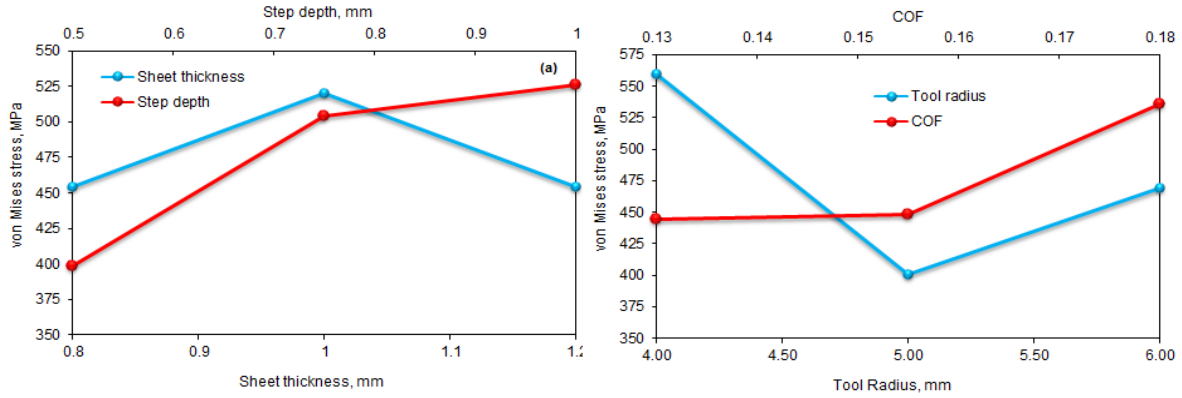

Figure 2: Influence of process parameters on von Mises stress.

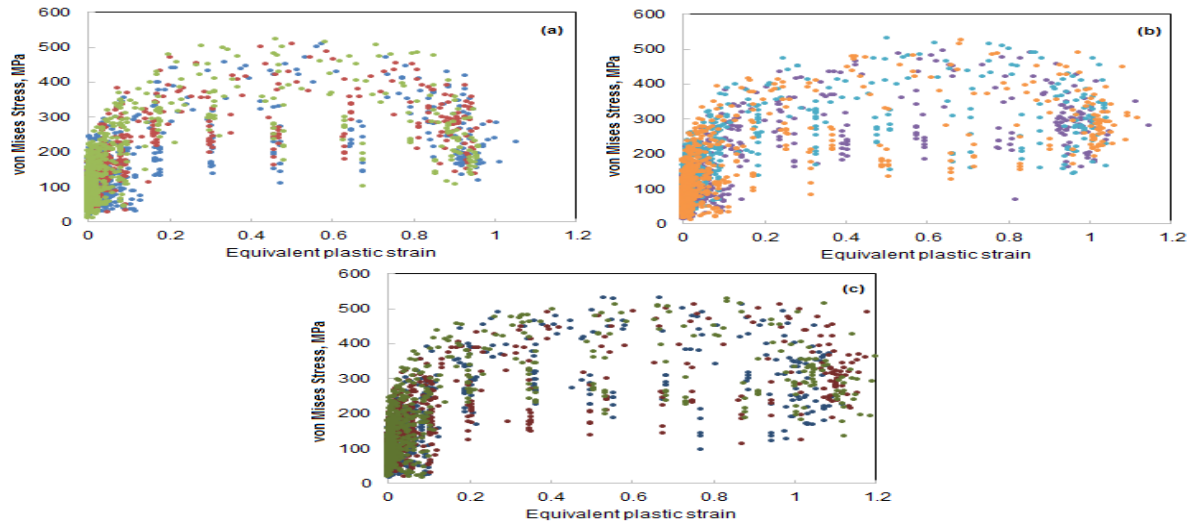

Figure 3: Effect of equivalent plastic strain on von Mises stress.

For the trials 1, 2 and 3, the von Mises stresses are, respectively, 428.50 MPa, 378.16 MPa and 557.36 MPa. For the trials 4, 5 and 6, the von Mises stresses are, respectively, 425.72 MPa, 508.60 MPa and 625.29 MPa. For the trials 7, 8 and 9, the von Mises stresses are, respectively, 341.09 MPa, 625.07 MPa and 396.89 MPa. The ultimate tensile strength of brass is 470 MPa For trials 1, 2, 4, 7 and 9 the von Mises stress is lower than the ultimate tensile strength of brass. For trials 3, 5, 6 and 8 which is nearer for trials 3 and 5 the von Mises stress id higher than the tensile strength of brass as shown in Fig.4.

International Journal of Advance Research in Science and Engineering
Vol. No.5, Issue No. 11, November 2016
www.ijarse.com
IJARSE
ISSN (O) 2319 - 8354
ISSN (P) 2319 - 8346

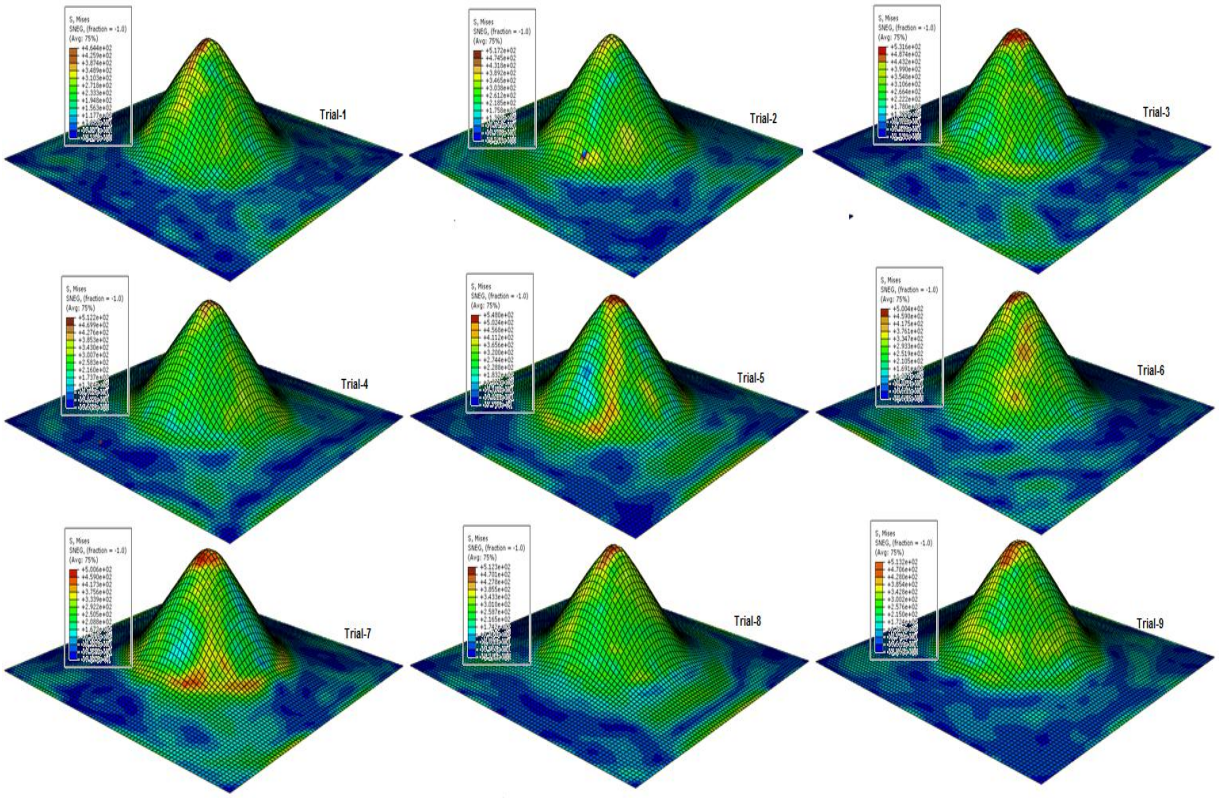

Figure 4: Raster images of von Mises stress in the cups.

3.2 Influence of parameters on strain rate

The ANOVA summary of the strain rate is given in Table 4. The percent contribution column establishes the major contributions 4.70%, 19.16%, 52.87% and 23.28% of sheet thickness, step depth, tool radius and coefficient of friction, respectively, towards variation in the strain rate.

Table 4: ANOVA summary of the strain rate

Source	Sum 1	Sum 2	Sum 3	SS	v	V	P
A	0.2899607	0.1826032	0.2656889	0.0021131	2	0.0010566	4.70
B	0.1186108	0.3368987	0.2827434	0.0086136	2	0.0043068	19.16
C	0.1509828	0.4635421	0.123728	0.0237677	2	0.0118839	52.87
D	0.27	0.3544409	0.1088919	0.0104648	2	0.0052324	23.28
e				6.939E-18	0		0
T	0.83	1.34	0.78	0.04	8		100.00

International Journal of Advance Research in Science and Engineering
Vol. No.5, Issue No. 11, November 2016
www.ijarse.com
IJARSE
ISSN (O) 2319 - 8354
ISSN (P) 2319 - 8346

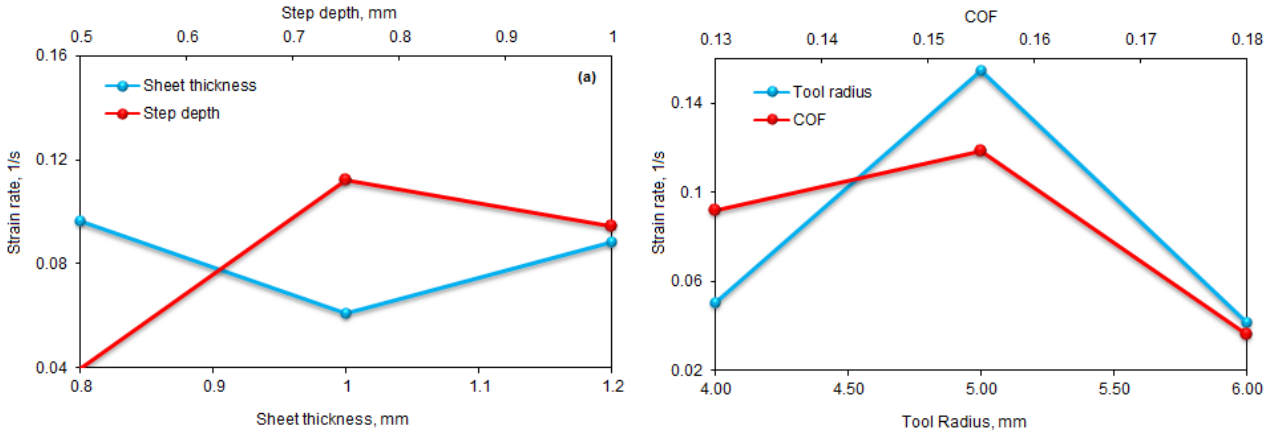

Figure 5: Influence of process variables on strain rate.

The strain rate as a function of sheet thickness and tool radius is shown in Fig.5a. The sheet thickness is the representative of the material availability for plastic deformation. The strain rate is low for the sheet thickness of 1.00 mm and it is high for step of 0.75 mm. The magnitude of the step (Δz) down that the tool made after each pass is an important parameter, which had an effect on the strain rate, which depends upon the elastic-plastic deformation of sheet. For smaller step size local deformation plays an important role than stretching. The strain rate is high for tool radius of 5.00 mm and friction coefficient of 0.15 as shown in figure 5b. The frictional shear stress is directly proportional to the coefficient of friction as per Coulomb's law of friction ($\tau = \mu F_n$, where F_n is the normal pressure). When the frictional shear stress, reaches the limiting shear stress of the sheet material, the material undergoes plastic deformation. From this point, the frictional shear stress does not increase and has the value of the limiting shear stress and thereby limiting the coefficient of friction. Therefore, at each contact spot of tool with sheet, the local strain determines the friction.

3.3 Influence of parameters on thickness reduction

The ANOVA summary of the thickness reduction is given in Table 5. The thickness reduction is highly influenced by the sheet thickness only. The influence of all other process variables is negligible towards variation in the thickness reduction.

Table 5: ANOVA summary of the thickness reduction

Source	Sum 1	Sum 2	Sum 3	SS	v	V	P
A	1.49	1.86	2.24	0.09	2.00	0.05	99.31
B	1.88	1.87	1.85	0.00	2.00	0.00	0.20
C	1.88	1.86	1.86	0.00	2.00	0.00	0.09
D	1.86	1.89	1.84	0.00	2.00	0.00	0.41
e				0.00	0.00		0.00
T	7.11	7.48	7.79	0.09	8.00		100.00

International Journal of Advance Research in Science and Engineering
Vol. No.5, Issue No. 11, November 2016
www.ijarse.com
IJARSE
ISSN (O) 2319 - 8354
ISSN (P) 2319 - 8346

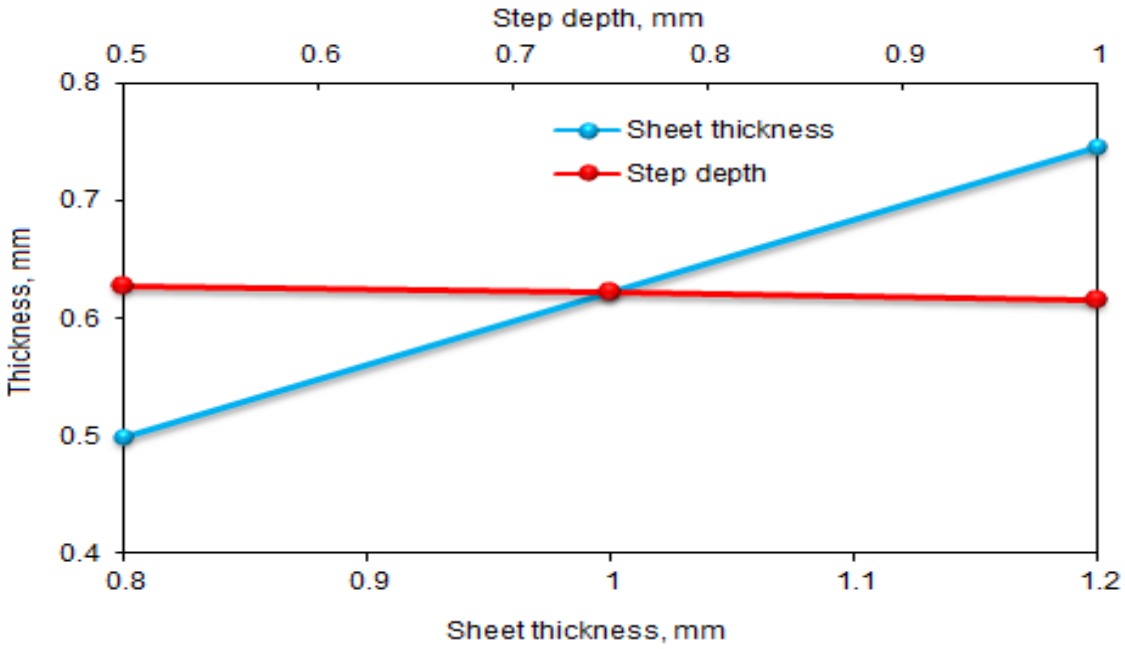

Figure 6: Influence of process parameters on thickness reduction.

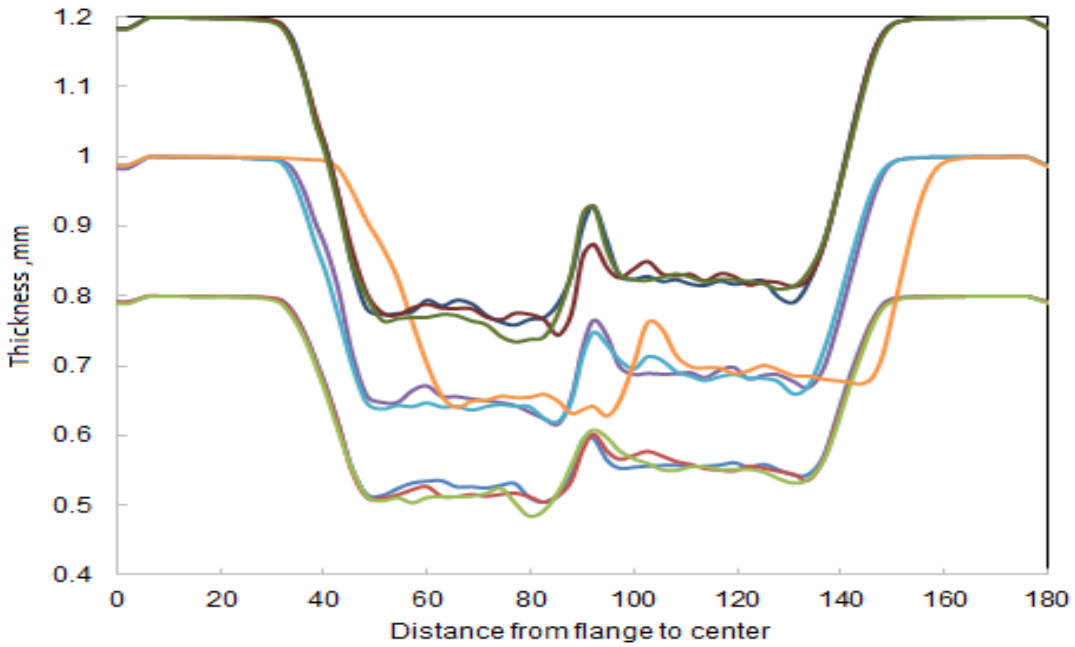

Figure 7: Location of thickness reduction in the deformed cup.

The reduction of sheet thickness is increased with increase of sheet thickness as shown in Fig.6. The reduction of thickness was considered at the centerline of the deformed cup as shown in Fig.7. As observed from Fig.7, the majority of thickness reduction takes place in the walls of the cup but not in the flange or bottom of the cup.

IJARSE
ISSN (O) 2319 - 8354
ISSN (P) 2319 - 8346

The elements located at the mid regions of the walls are elongated higher than those present at the top and bottom of the cup walls.

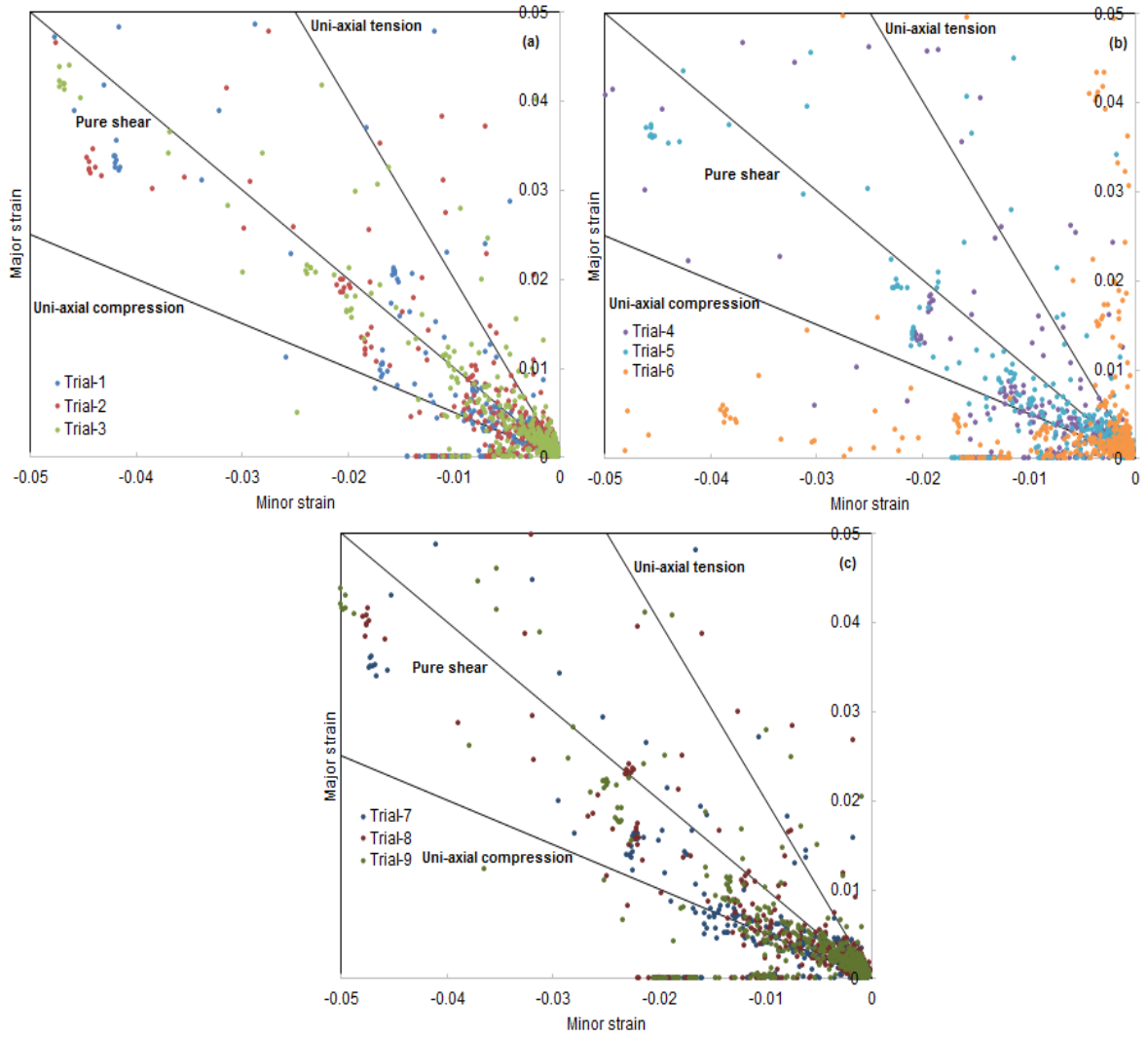

Figure 8: Forming limit diagrams (a) for trials 1, 2, 3 (b) for trials 4, 5, 6 (c) for trials 7, 8, 9.

3.4 Formability of SPIF process

The formability diagrams of the hyperbolic cups are shown in Fig.8a-c. During initial stages of SPIF, the shear and compressive stresses were dominating the formability of hyperbolic cups of brass. At later stages of plastic deformation, the tension is highly predominant resulting the stretching sheet. For trials 1, 2, 3, 7, 8 and 9 the formability is influenced by the pure shear and uniaxial tension while it is effected by tension and compression for trails 4, 5 and 6.

IJARSE
ISSN (O) 2319 - 8354
ISSN (P) 2319 - 8346

IV.CONCLUSIONS

The major SPIF process parameters, which influence the formability of hyperbolic cups of brass, were step size, coefficient of friction and tool radius. The reduction of thickness was highly influenced by the sheet thickness only. The optimal process variables could be any combination of trails 7, 8 and 9 for producing successful cups.

REFERENCES

[1] A. E. Tekkaya, A guide for validation of FE-simulations in bulk metal forming, The Arabian Journal for Science and Engineering. 30, 2005, 113-136.

[2] A. C. Reddy, Formability of Warm Deep Drawing Process for AA1050-H18 Rectangular Cups, International Journal of Mechanical and Production Engineering Research and Development, 6(4), 2015, 85-97.

[3] A. C. Reddy, Formability of High Temperature and High Strain Rate Superplastic Deep Drawing Process for AA2219 Cylindrical Cups, International Journal of Advanced Research, 3(10), 2015, 1016-1024.

[4] A. C. Reddy, Practicability of High Temperature and High Strain Rate Superplastic Deep Drawing Process for AA3003 Alloy Cylindrical Cups, International Journal of Engineering Inventions, 5(3), 2016, 16-23.

[5] A.C. Reddy, Finite element analysis of reverse superplastic blow forming of Ti-Al-4V alloy for optimized control of thickness variation using ABAQUS, Journal of Manufacturing Engineering, 1(1), 2006, 6-9.

[6] A. C. Reddy, T. K. K. Reddy, M.Vidya Sagar, Experimental characterization of warm deep drawing process for EDD steel, International Journal of Multidisciplinary Research & Advances in Engineering, 4(3), 2012, 53-62.

[7] A. C. Reddy, Evaluation of local thinning during cup drawing of gas cylinder steel using isotropic criteria, International Journal of Engineering and Materials Sciences, 5(2), 2012, 71-76.

[8] V. Srija, A. C. Reddy, Numerical Simulation of Truncated Pyramidal Cups of AA1050-H18 Alloy Fabricated by Single Point Incremental Forming, International Journal of Engineering Sciences & Research Technology, 5(6), 2016, 741-749.

[9] T. Santhosh Kumar, A. C. Reddy, Single Point Incremental Forming and Significance of its Process Parameters on Formability of Conical Cups Fabricated From AA1100-H18 Alloy, International Journal of Engineering Inventions, 5(6), 2016, 10-18.

[10] A. Raviteja, A. C. Reddy, Implication of Process Parameters of Single Point Incremental Forming for Conical Frustum Cups From AA 1070 using FEA, International Journal of Research in Engineering and Technology, 5(6), 2016, 124-129.

[11] T. Santhosh Kumar, V. Srija, A. Ravi Teja, A. C. Reddy, Influence of Process Parameters of Single Point incremental Deep Drawing Process for Truncated Pyramidal Cups from 304 Stainless Steel using FEA, International Journal of Scientific & Engineering Research, 7(6), 2016, 100-105.

[12] C. R. Alavala, FEM Analysis of Single Point Incremental Forming Process and Validation with Grid-Based Experimental Deformation Analysis, International Journal of Mechanical Engineering, 5(5),2016, 1-6.

IJARSE
ISSN (O) 2319 - 8354
ISSN (P) 2319 - 8346

[13] C. R. Alavala, Validation of Single Point Incremental Forming Process for Deep Drawn Pyramidal Cups using Experimental Grid-Based Deformation, International Journal of Engineering Sciences & Research Technology, 5(8), 2016, 481-488.

[14] C. R. Alavala, CAD/CAM: Concepts and Applications, New Delhi: PHI Learning Pvt. Ltd, 2008.